ELSEVIER

Fusion Engineering and Design 42 (1998) 299–305

Fusion Engineering and Design

# Integral experiment of induced radioactivity in D-T fusion neutron environment and validation of activation cross section library

Y. Kasugai [a,*], Y. Ikeda [a], F. Maekawa [a], C. Konno [a], M. Wada [a], Y. Uno [a],
A. Kumar [b], M.Z. Youssef [b], M.A. Abdou [b]

[a] *Fusion Neutronics Laboratory, Department of Reactor Engineering, Japan Atomic Energy Research Institute, Tokai-mura, Ibaraki-ken 319-11, Japan*
[b] *Mechanical, Aerospace, and Nuclear Engineering Department, School of Engineering and Applied Science, 43–133, Engineering-lV, 405 Hilgard Avenue, University of California at Los Angeles (UCLA), Los Angeles, CA 90095-159710, USA*

## Abstract

Under ITER/EDA R&D Task T-218, an integral experiment on the induced radioactivity was conducted at the Fusion Neutronics Source (FNS) facility in JAERI. The objective was to provide experimental data for validating the inventory calculation codes and relevant activation cross section libraries to be used in the ITER nuclear design. Sample materials investigated were Al, Mg, Ti, V, Mn, Fe, Ni, SS-316LN, Cu, Zn, Nb, Mo, Ag, In, Sn, Hf, Ta, W and Pb. The corresponding neutron spectra at two locations were calculated by MCNP4A with JENDL-Fusion File based nuclear data library by modeling the experimental assembly precisely. The calculations with currently updated activation cross sections, JENDL-ACT96, FENDL-A1 and FENDL-A2, were carried out to compare the results with the experiment. The results for the comparison between the measurement and calculation of radioactivity are discussed in terms of the adequacy of calculation as far as the D-T neutron dominated neutron field is concerned.

## 1. Introduction

The importance of the induced radioactivity in a D-T fusion environment is recognized as the most critical issue from a safety point of view [1–5]. In order to arrive at an establishing qualified data base for the design calculation, extensive efforts have been carried out in terms of inventory calculation code development and associated data library preparations [6–14]. ITER development have addressed important tasks undertaken in the R&D to validate all processes requested for the design calculation. The requirement for the reactor licensing order has been noted. In order to make all efforts for the code system development effective, validation with experimental data are highly necessary to assure objectively the reliability of the calculation values themselves. For this purpose, integral experiments demonstrated effectiveness by means of showing the quality of the cross section data and calcula-

---

* Corresponding author. Fax: +81 29 2825709; e-mail: kasugai@fnshp.tokai.jaeri.go.jp

0920-3796/98/$19.00 © 1998 Elsevier Science S.A. All rights reserved.
*PII* S0920-3796(98)00099-4

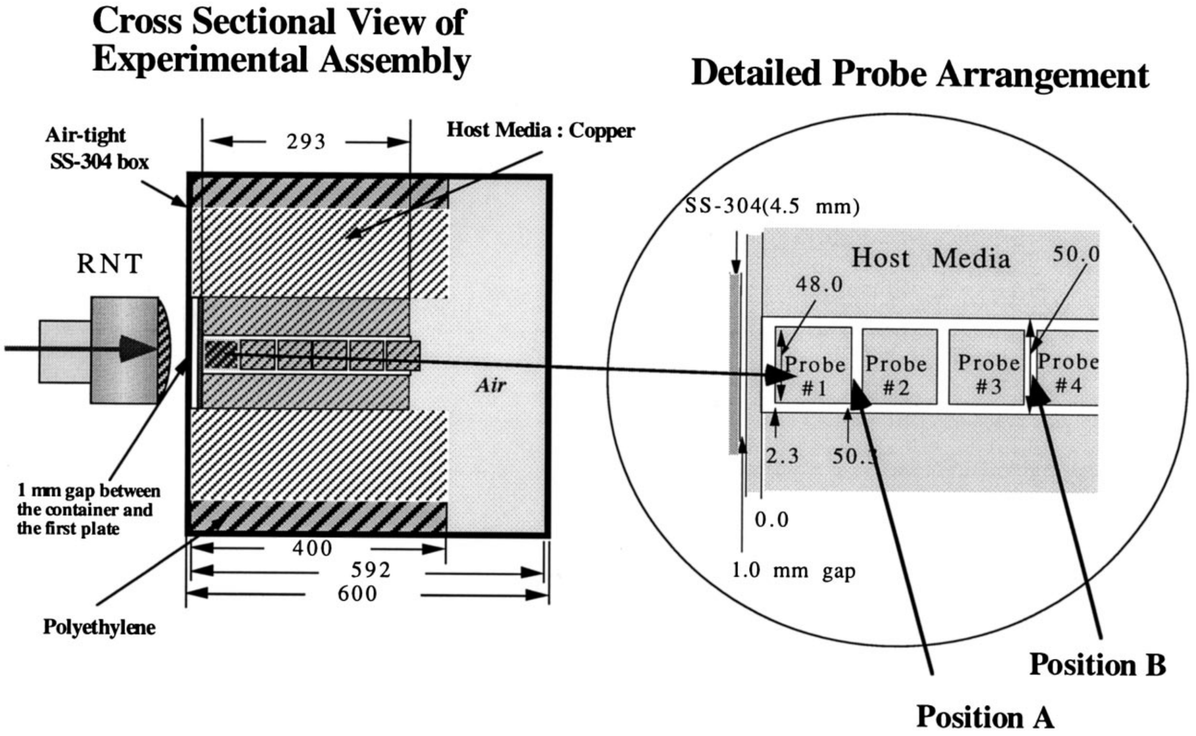

Fig. 1. Cross sectional view of the copper assembly and sample position.

Table 1
List of irradiation time, neutron yield, used materials and cooling time

| No. | Irradiation time (h) | Neutron yield | Material | Cooling time |
|---|---|---|---|---|
| 1 | 4 | $2.93 \times 10^{16}$ | Fe, Ni, Cu, Co, Mg, Ti, W, Hf, Sus | 12 h–100 d |
| 2 | 4 | $2.68 \times 10^{16}$ | Ag, Ta, V, Sn, Dy, Pb | 4 h–100 d |

tion method and relevant decay data. The importance was demonstrated by an extensive experimental program on the induced radioactivity under the framework of JAERI/USDOE collaboration [15,16]. The program provided invaluable knowledge regarding the present status of the cross section adequacy through experimental analysis. The radioactivities of concern, however, were products of near threshold type reaction with D-T neutrons, and these, as a result of the tested neutron spectra, were rather hard. However, there have been critical needs to execute experiments with neutron spectra where a D-T primary neutron is insignificant compared to the low energy neutrons. Uncertainty from the neutron spectrum calculation has not been verified thoroughly and was left to be examined.

This paper describes a new integral experiment on the induced radioactivity in copper assemblies. Two irradiation positions with different neutron spectra were selected. The primary objective of these experiments is to provide integral experimental data of induced radioactivity to validate the data and method associated with various materials of Al, Mg, Ti, V, Mn, Fe, Ni, SS-316LN, Cu, Zn, Nb, Mo, Ag, In, Sn, Hf, Ta, W and Pb, which are expected to be used in a fusion reactor. The parameters investigated were cooling time, neutron spectrum, cross section libraries, which

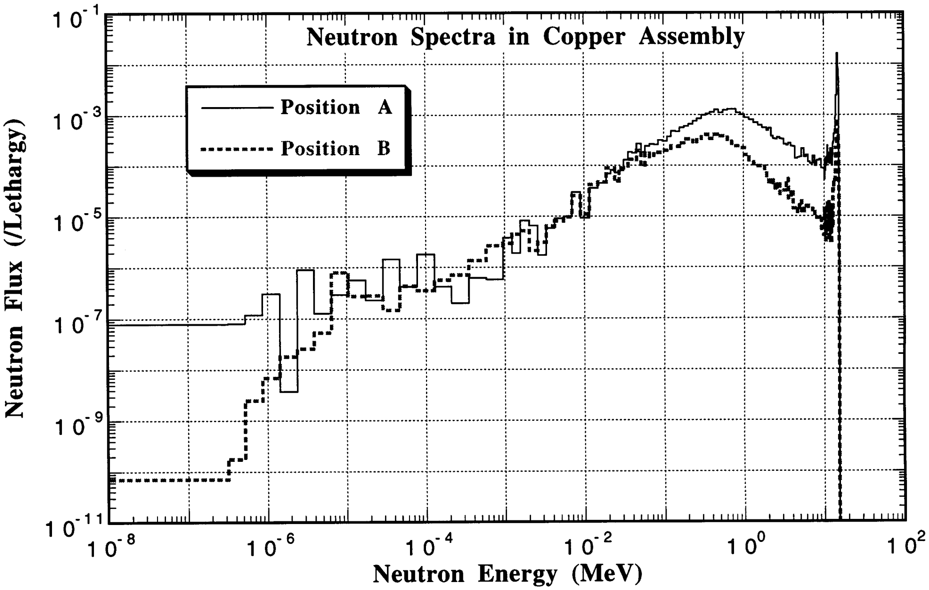

Fig. 2. Neutron flux spectra at positions A and B, calculated by MCNP-4A with FSXLIB-J3.2 nuclear data library.

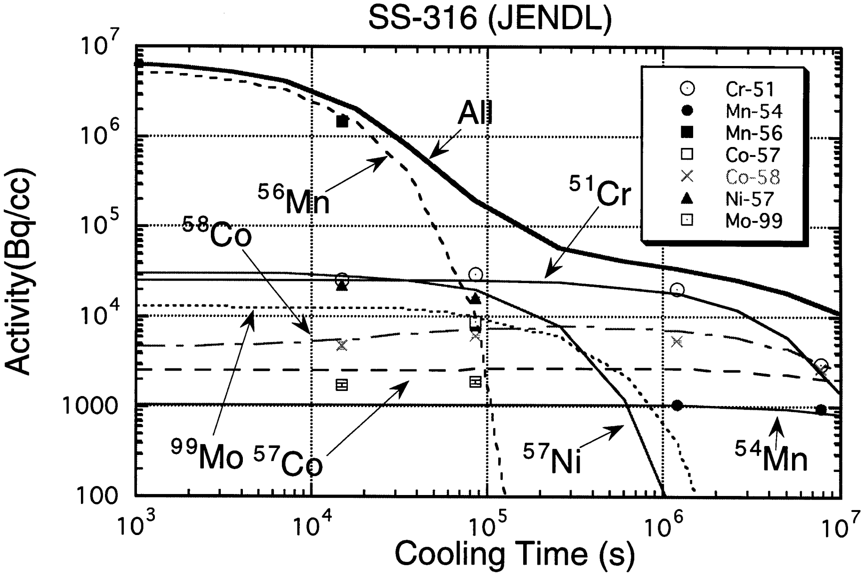

Fig. 3. Measured radioactivities at position A at different cooling times and corresponding decay curves calculated with ACT4/JENDL-ACT96.

should be factored into consideration in the experimental analysis. As the neutron transport code, a continuous energy Monte Carlo code MCNP-4A [17] was employed coupled with FSXLIB-J3.2 [18] and FENDL-MC based on JENDL-3.2 nuclear data file [19] and FENDL/E1 [20], respectively. For the activation calculations, ACT4 of THIDA code system [7] with JENDL activation library [14], FENDL-A1[12] and FENDL-A2activation library [13] was used.

Table 2
C/E values for induced radioactivities in various materials

| C/E | | | | | | | |
|---|---|---|---|---|---|---|---|
| Material | Product | Position A | | | Position B | | |
| | | JENDL | FENDL/A1 | FENDL/A2 | JENDL | FENDL/A1 | FENDL/A2 |
| SS-316 | $^{57}$Co | 1.39 | 1.39 | 1.39 | 1.32 | 1.26 | 1.25 |
| | $^{51}$Cr | 0.93 | 0.93 | 0.94 | 0.94 | 0.86 | 0.91 |
| | $^{56}$Mn | 1.18 | 1.79 | 1.08 | 1.00 | 2.89 | 0.93 |
| | $^{58}$Co | 1.07 | 1.09 | 1.12 | 1.07 | 1.09 | 1.36 |
| | $^{54}$Mn | 0.91 | 0.95 | 0.97 | 0.80 | 0.80 | 0.84 |
| | $^{57}$Ni | 1.19 | 1.20 | 1.09 | 1.19 | 1.14 | 1.03 |
| | $^{99}$Mo | 1.07 | 1.06 | 1.04 | 0.98 | 0.93 | 0.95 |
| Mg | $^{24}$Na | 1.15 | 1.12 | 1.14 | 1.13 | 1.09 | 1.11 |
| Ti | $^{46}$Sc | 1.31 | 1.22 | 1.12 | 1.34 | 1.32 | 0.79 |
| | $^{47}$Sc | 1.22 | 1.46 | 1.24 | 1.76 | 1.76 | 1.44 |
| | $^{48}$Sc | 1.17 | 1.17 | 1.01 | 1.45 | 1.39 | 1.19 |
| V | $^{48}$Sc | 0.97 | 0.96 | 0.96 | 0.81 | 0.98 | 0.98 |
| Fe | $^{56}$Mn | 1.08 | 1.14 | 1.08 | 1.06 | 1.07 | 1.02 |
| | $^{54}$Mn | 1.18 | 1.16 | 1.23 | 1.16 | 1.12 | 1.17 |
| | $^{51}$Cr | 0.83 | 0.88 | 0.83 | — | — | — |
| Co | $^{58}$Co | 0.54 | 1.02 | 1.02 | 0.57 | 1.00 | 0.99 |
| | $^{56}$Mn | 1.02 | 0.94 | 0.97 | 1.01 | 0.89 | 0.92 |
| | $^{59}$Fe | 1.03 | 1.54 | 1.03 | 1.12 | 1.60 | 1.10 |
| Ni | $^{57}$Co | 0.99 | 0.94 | 0.94 | 0.93 | 0.83 | 0.83 |
| | $^{57}$Ni | 0.99 | 1.11 | 1.01 | 0.92 | 0.99 | 0.89 |
| | $^{58}$Co | 1.21 | 1.12 | 1.15 | 1.10 | 0.96 | 1.25 |
| | $^{61}$Co | 1.50 | 1.93 | 2.20 | 1.56 | 1.90 | 2.17 |
| | $^{60}$Co | 0.97 | 1.03 | 1.03 | — | — | — |
| Cu | $^{65}$Ni | 1.19 | 1.06 | 1.19 | 1.16 | 1.02 | 1.12 |
| | $^{64}$Cu | 1.04 | 1.01 | 1.01 | 1.35 | 1.20 | 1.19 |
| Ag | $^{106m}$Ag | 1.13 | 1.13 | 1.13 | 0.82 | 0.82 | 0.77 |
| | $^{106m}$Rh | 0.09 | 0.18 | 0.15 | 0.54 | 0.54 | 0.44 |
| | $^{110}$Ag | 0.12 | 4.31 | 0.74 | — | — | — |
| Sn | $^{117g}$In | 1.61 | 1.74 | 0.39 | 0.63 | 0.60 | 0.75 |
| | $^{117m}$In | 0.77 | 0.78 | 1.00 | — | — | — |
| | $^{117m}$Sn | 1.12 | 1.12 | 0.90 | 1.26 | 1.21 | 0.90 |
| | $^{123m}$Sn | 0.79 | 0.79 | 0.80 | 0.69 | 0.66 | 0.71 |
| | $^{111g}$In | 1.15 | 1.15 | 0.80 | 1.28 | 1.21 | 1.11 |
| | $^{113g}$Sn | 0.77 | 0.76 | 0.78 | 0.72 | 0.71 | 0.73 |
| Dy | $^{165}$Dy | 0.17 | 0.16 | 0.16 | 1.21 | 1.17 | 1.16 |
| | $^{157}$Dy | 1.32 | 1.32 | 1.32 | 0.42 | 0.40 | 0.40 |
| Hf | $^{180m}$Hf | — | 15.10 | 1.82 | 1.43 | 12.71 | 1.47 |
| | $^{181}$Hf | 1.33 | 1.21 | 1.15 | 1.11 | 1.04 | 1.12 |
| | $^{179m}$Hf | 0.14 | 0.95 | 0.24 | 1.28 | 35.5 | 2.48 |
| Ta | $^{182}$Ta | 1.26 | 1.25 | 0.88 | 1.02 | 1.21 | 0.90 |
| | $^{180}$Hf | 0.94 | 0.97 | 0.03 | — | — | — |
| W | $^{187}$W | 0.59 | 1.12 | 1.16 | 0.69 | 0.72 | 0.74 |
| Pb | $^{203}$Pb | *** | *** | 1.02 | *** | *** | 1.04 |
| | $^{204m}$Pb | *** | *** | 1.52 | *** | *** | 0.85 |

—, No experimental data available; ***, no corresponding calculations.

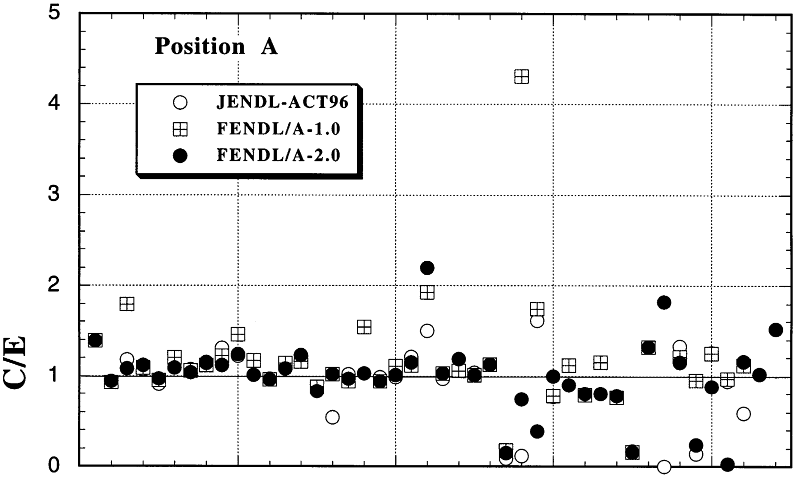

Fig. 4. Overall C/E for radioactivities at position A.

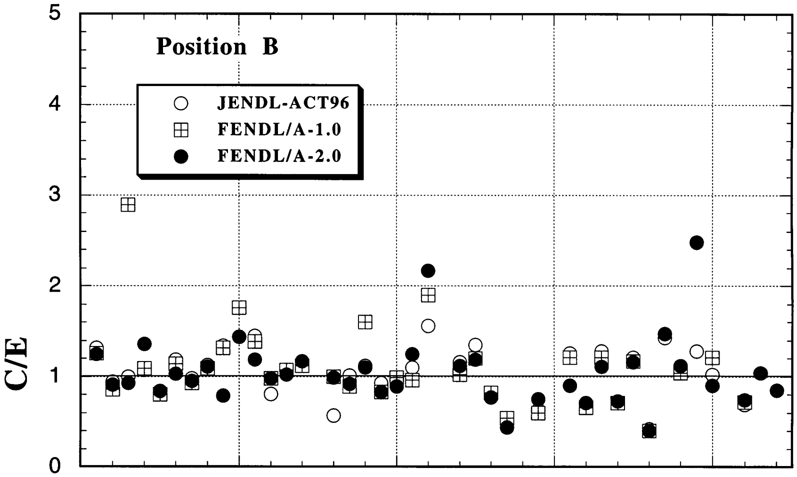

Fig. 5. Overall C/E for radioactivities at position B.

## 2. Experiment

### 2.1. Neutron source

The D-T neutrons were generated by bombarding a tritiated rotating target with a 20 mA deuteron beam accelerated to 350 kV at FNS [21]. The absolute neutron yield was monitored by a $^{232}$Th fission chamber which was calibrated by the associated alpha-particle counting method. Nominal neutron yield at the target was $3–4 \times 10^{12}$ ns$^{-1}$. The D-T neutron target was located at the center of the target room with the dimensions $5 \times 5 \times 4.5$ m, surrounded by ordinary 2.5-m thick concrete walls. The neutron irradiation history was recorded with multichannel scaling (MCS) with 10 s duel time bin.

### 2.2. Experimental assembly

The schematic cross sectional views of the experimental assembly are given in Fig. 1. The central zone of the assembly consisted of copper blocks with a central channel hole of 50 mm in diameter. The cross section of the central zone of copper measured 150 × 150 mm. In addition to this central region, ≈100 mm thick copper regions were stacked, followed by a 100 mm polyethylene layer. The outer dimension of the container was 600 × 600 × 600 mm. The assembly was set in front of the D-T neutron target as the distance between the target outer surface, and the front surface of the assembly was 14 mm. The axis of the central channel was aligned to the $d^+$ beam direction in order to keep good symmetric configuration. The height of the $d^+$ beam line was 1.8 m from the ground floor.

### *2.3. Sample materials, irradiation and measurement*

The samples of Al, Mg, Ti, V, Mn, Fe, Ni, SS-316LN, Cu, Zn, Nb, Mo, Ag, In, Sn, Hf, Ta, W and Pb were irradiated with D-T neutrons at two positions in the copper assembly, namely, position A at 50.2 mm from the bottom of the experimental channel and position B at 151.2 mm. The size of the sample is 10 × 10 × 0.01–0.5 $mm^3$. The weight of the sample ranged from 10 to 300 mg.

After irradiation, induced radioactivities were measured by $\gamma$-ray spectroscopy with Ge detectors at cooling time from several minutes to about one year. Experimental data were derived as the radioactivity intensity per unit volume (Bq $cm^{-3}$). The radioactivities were identified by $\gamma$-ray energies and their intensity relationship. The decay rate was derived from $\gamma$-ray counts, detector efficiency, $\gamma$-ray emission probability and other corrections needed, e.g. $\gamma$-ray collection time, half-lives, etc. The decay property data were taken from the Table of Radioactive Isotopes [22]. When there were multiple $\gamma$-rays associated with a particular radionuclide, the most intense $\gamma$-ray line was used for the data processing. In Table 1, irradiation, materials, neutron yield, and typical cooling times are summarized.

## 3. Experimental analysis

A 3D code, MCNP-4A [17], was used for modeling the rotating target geometry and the experimental assembly. The library, FSXLIB-J3.2 [18], was used for neutron transport in MCNP calculation in the whole system. Neutron spectra at two locations, A and B, were calculated (Fig. 2). Also, FENDL-1 library was applied for the MCNP calculation. The neutron spectra obtained by the two libraries were almost identical.

The ACT4 of the THIDA code system [7] was used as the radioactivity inventory codes. The activation cross section library based on the JENDL-ACT96 [14] activation file with 125 neutron energy groups (JENDL) and FENDL-A1 [12] and FENDL-A2 [13] with 175 neutron energy groups were used for the induced radioactivity calculations. Induced radioactivities corresponding to the experimental conditions were calculated by those codes to be compared with the measured value. Fig. 3 shows decay profiles for radioactivities induced in SS-316 irradiated at position A, calculated using JENDL along with the experimental data.

## 4. Results and discussion

The induced radioactivities given in Bq $cm^{-3}$ at each cooling time were compared with calculations. The ratios of the calculation to the experiment (C/E) are tabulated in Table 2. In general, there is good agreement for the radioactivities in which activation cross sections are well known. These good agreements indicated that the calculated neutron spectra were reasonably validated to be used in the radioactivity analysis. For example (Fig. 3), there are excellent one-to-one correspondences of the measurements to calculations for the SS316 case. However, overestimations and underestimations by more than a factor of 2, were found in the calculations for some important radioactivity productions. For example, all calculations overestimated $^{24}Na$ production in Mg by a factor of 2. For $^{110m}Ag$ production in Ag via the $^{109}Ag(n,\gamma)^{110m}Ag$ reaction, JENDL and FENDL-A1 gave an underestimation and an overestimation by more than a factor of 4, respectively, whereas FENDL-A2 gave a reasonable agreement with C/E of 0.74. There were underestimations in all of the calculations for $^{165}$Dy production at position A, whereas calculations gave reasonable agreements with the measurement at position B. For $^{180}$Hf production, JENDL and FENDL-A2 gave better results than FENDL-A1. For $^{179m}$Hf production, JENDL and FENDL-A2 were much better than FENDL-A1, though they still overestimated the measurement. In general, however, (Figs. 4 and 5), FENDL-A2 showed better agreement with the experiment that JENDL and FENDL-A1. This fact is the direct demonstration of the FENDL-A2 quality, which has been completed through a stringent selection procedure by the international collaboration.

## 5. Summary

The integral test of the induced radioactivity calculation has been carried out using neutron spectra in the copper assembly bombarded with 14 MeV neutrons. The results ensured an improved FENDL-A2 quality. However, further investigation for the activation of cross sections for minor elements to be used in the fusion reactor components is still required.

## Acknowledgements

The authors wish to acknowledge J. Kusano, C. Kutsukake, S. Tanaka, Y. Abe for the operation of the FNS accelerator.

## References

[1] R.W. Conn, E.E. Bloom, J.W. Davis, R.E. Gold, R. Little, K.R. Schultz, D.L. Smith, F.W. Wiffen, Lower activation materials and magnetic fusion reactors, Nucl. Technol. Fusion 5 (1984) 291.

[2] G. Logan, A rationale for fusion economics based on inherent safety, J. Fusion Energy 4 (1985) 245.

[3] E.T. Cheng, Radioactivity aspects of fusion reactors, Fusion Eng. Des. 8 (1989) 10.

[4] M. Zucchetti, Impurity concentration limits and activation in fusion reactor structural materials, Fusion Technol. 19 (1991) 294.

[5] E.T. Cheng, K.M. Feng, R. Forrest, J.H. Huang, J. Kopecky, F.M. Mann, A.V. Kasirskij, D.V. Markovskij, O. Schipakin, M. Sawan, Y. Seki, International fusion activation calculation comparison study, TSIR-12 (1991).

[6] F.M. Mann, REAC*2: Users manual and code description, WHC-EP-0282, Westinghouse Hanford (1989).

[7] Y. Seki, H. Iida, H. Kawasaki, K. Yamada, THIDA-2: An advanced code system for calculation of transmutation, activation, decay heat and dose rate, RSIC computer code collection, CCC-410 (April 1987).

[8] D.L. Henderson, O. Yasar, A radioactivity and dose rate calculation code package, vols. 1 and 2, RSIC computer code collection, CCC-323 (April 1987).

[9] J. Jung, Theory and use of the radioactivity code RACC, ANL/FPP/TM-122, Argonne National Laboratory (1979).

[10] Y. Nakajima, JENDL activation cross section file, JAERI-M 91-032 (1991) 43–57.

[11] F.M. Mann, REAC*3 nuclear data libraries, Proc. International Conference on Nuclear Data for Science and Technology, Juelich, Germany, 12–17 May 1991, pp. 936–938.

[12] A.B. Pashchenko, Status of FENDL activation file and plans for the future developments, Proc. International Workshop on Nuclear Data for Fusion Reactor Technology, Del Mar, California, 3–6 May 1993.

[13] A.B. Pashchenko, Completion of FENDL-1 and start of FENDL-2, IAEA NDC, report, INDS(NDS)-325 (1996).

[14] Y. Nakajima, T. Asami, T. Watanabe, N. Yamamuro, K. Maki, Y. Ikeda, S. Iwasaki, M. Yan, Y. Seki, to be published in JAERI-Report (1998)

[15] A. Kumar, Y. Ikeda, M.A. Abdou, M.Z. Youssef, K. Konno, K. Kosako, Y. Oyama, T. Nakamura, H. Maekawa, Decay radioactivity induced in plasma facing component materials by deuterium-tritium neutrons, Fusion technol. 28 (1) (1995) 99.

[16] Y. Ikeda, A. Kumar, C. Konno, K. Kosako, Y. Oyama, F. Maekawa, M.Z. Youssef, M.A. Abdou, Measuremements and analyses of decay radioactivity induced in simulated deuterium-tritium neuron environments for fusion reactor structural materials, Fusion Technol. 28 (1) (1995) 74.

[17] J.F. Briesmeister (Ed.), MCNP–A general Monte Carlo N-particle transport code, Version 4A, LA-12625-M, Los Alamos National Laboratory (1993).

[18] K. Kosako, F. Maekawa, Y. Oyama, Y. Uno, H. Maekawa, FSXLIB-J3R2: A continuous energy cross section library for MCNP based on JENDL-3.2, JAERI-Data/Code 94-020, JAERI (1994).

[19] K. Shibata, et al., Japanese evaluated nuclear data library, Version-3, JAERI-1319 (1990).

[20] S. Ganesan, H. Wienke, FENDL/MC-1.0 library of continuous energy cross sections in ACE format for neutron–photon transport calculations with the Monte Carlo neutron and photon transport code system MCNP 4A, IAEA-NDS-169, I.A.E.A. (1995).

[21] T. Nakamura, H. Maekawa, J. Kusano, Y. Oyama, Y. Lkeda, C. Kutsukake, S. Tanaka, Shu. Tanaka: Present status of the fusion neutron source (FNS), Proc. 4th Symp. on Accelerator Science and Technology, RIKEN, Saitama, 24–26 November (1982) 155-156.

[22] E. Browne, R.B. Firestone, V.S. Shirley (Ed.), Table of Radioactive Isotopes, Wiley, New York, 1986.